Responsible (Name, Organisation) Massimo Ceraolo – Università Pisa	DELIVERABLE REPORT		Page 1(24)
Issuer (Name, Organisation) Massimo Ceraolo – Università Pisa	Date 10.5.2013	WP No 3200	Report No D.3200.5
Subject Preliminary model for Li cell			Dissem. Level **PU**

Deliverable 3200.5

Preliminary model definition for Li cell

Summary

This deliverable discusses the details of the mathematical model developed for the project's lithium cells, based on experimental results, which was planned as part of WP3200 "Basic storage system testing and modelling", in Task 3230 "Modelling", with the scope to develop and validate, with experimental test work, dedicated mathematical models for Li and SC cells. The developed model can be also useful for control strategy on modules and final battery system.
The structure of the model and all the numerical values of the parameters for HCV Li cells have been analysed and developed by using experimental results obtained at Pisa's laboratories.

In this report, a Li cell model, with its numerical parameters, has been selected from the initial list, critically prepared in the first year of the project, experimentally verified. Finally, the model has been used as the basis of a model-based State-of-Charge estimator, whose algorithm is described in detail in Deliverable D3200.7 [1].

Table of Contents

List of figures

List of tables

.

Nomenclature

1. Acronyms

LFP Lithium Iron Phosphate Cathode for Li cell
MST Multiple-Step test
NMC nickel manganese cobalt (a Li cell chemistry, based on the cathode composition)
OCV Open-Circuit Voltage
SOC State-of-Charge

2. Other quantities

C_n rated battery capacity (e.g. in Ah)
I_t Main-branch battery current
R_0 Algebraic battery internal resistance
R_i (*i= 1, 2, ….*) i-block battery internal resistance
C_i (*i= 1, 2, …..*) i-block battery internal capacitance
C_n Nominal capacity (batteries), nominal capacitance (supercapacitors)
θ inner cell temperature
θ_a ambient temperature
U_{oc} Open-circuit voltage *(same as OCV)*

Introduction

In Deliverable D3100.5 [2] discussion of mathematical models available for electrochemical batteries in general, and lithium batteries in particular was presented.

A general structure was defined, that allowed different degrees of precision, depending on the number of *R-C* blocks used for the electric model.

Figure 1 shows this general structure, with slight modification of symbols with respect to the version used in D3100.5.[1] Indeed this is a family of models, depending on number *n*: the higher this value, the higher the model's precision, but also the models complexity.

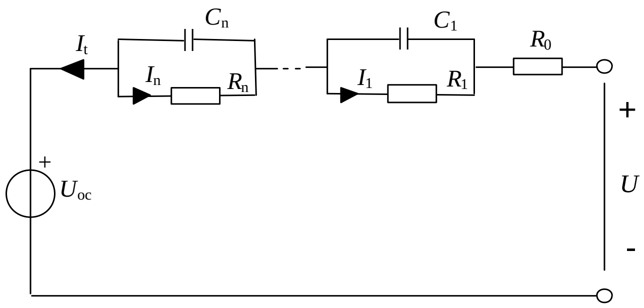

Figure 1. Generic structure of electric model of lithium cell (1st form).

This model can be used as a graphical-mathematical model of the cell's behaviour.
Its usage is not limited to off-line studies of the cell's behaviour, but it can be also very important in facilitating the determination of the cell's SOC, using Luenberger-style techniques, as detailed in the section named "Luenberger state estimator" of deliverable D3100.5.

In fact, it was shown in the section named "SOC models and evaluation" of D3100.5, while some lithium chemistries (as NMC chemistry) allow for an easy SOC determination by Ampere-hour counting and error correction using SOC-OCV correlation, the cells to be considered in this project show a behaviour that prevents this simple technique to be adopted.

Therefore detailed experimental evaluations of a sample, the considered nanostructrured LFP Li cells of the project, must be made, the parameters of the chosen model have to be determined, and verification of the model quality evaluated.
Based on this model, an SOC estimator based on a Luenberger-style estimator and an Extended Kalman filter will be defined, and this with its algorithm is presented in Deliverable D3200.7 [1].

The full definition of Li cell behaviour in HCV has to be performed according to the following steps:

1. <u>Verification of the applicability</u> of the general model, whose circuital description is shown in Figure 1, to the lithium cells chosen for HCV demonstrators;

---

1 The new symbol U_{oc} substitutes E_m, since the "oc" subscripts clearly shows that U_{oc} is the Open-Circuit voltage (after stabilisation).

2. Detailed definition of the cell's mathematical model. It relates to the need of choosing a unique structure from the family of circuits shown in figure 1, i.e. to determine the number *n* of R-C blocks;
3. Detailed definition of model's numerical parameters (values of E, R's, C's) at different values of SOC.

The next section of this deliverable in principle follows this order. However, an introductory section about the temperature span is also introduced to discuss some experimental results and decisions made during year 2012.

Technical progress

The cell

While D3100.5 [2] dealt with cell modelling in general, this document specifically addresses the Li cell and the related chemistry (nanostructured LFP cathode) chosen for the HCV project. The basic characteristics of this cell, as reported by the manufacturer, are described in Table 1.

Table 1. Basic Li cell technical characteristics.

Type	LFP -
Capacity (Ah)	4,4
Nominal voltage (V)	3,3
Max/min voltage (V)	3,8/1,6
Mass (kg)	0,205
Energy (Wh)	14,5
Specific Energy (Wh/kg)	70
discharge Power (W)*	550
Specific power (W/kg)	2700

These characteristics are nominal values, referred to defined operating measuring conditions.
Regarding specific power, further information can be drawn from the plot presented in Figure 2, supplied by the manufacturer.

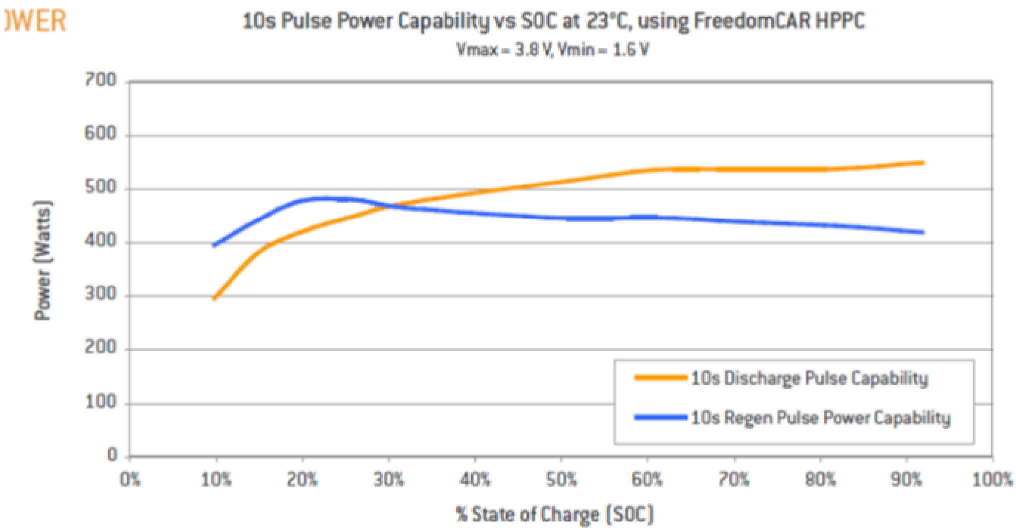

Figure 2. Power graph of the selected Li cell, supplied by the manufacturer.

Temperature span

The test cell matrix for the lithium cells was developed during the first year of the project and reported in Deliverable D3100.5 [2], section "Result and Discussion | Li battery test matrices". For clarity and completeness, the proposed test sequence for Li cells is reported again in Table 2.

Table 2. Test matrix at different temperatures for Li cells.

temperature/°C test		-15	0	20	40
Sequence 1	charge-based MST	x	x	x	x
Sequence 2	discharge-based MST-	x	x	x	x

Based on this test matrix, preliminary tests at different temperatures were performed on some HCV Li cells.
The results of charge and discharge behaviour at a current of 38 A are shown in Figure 3.

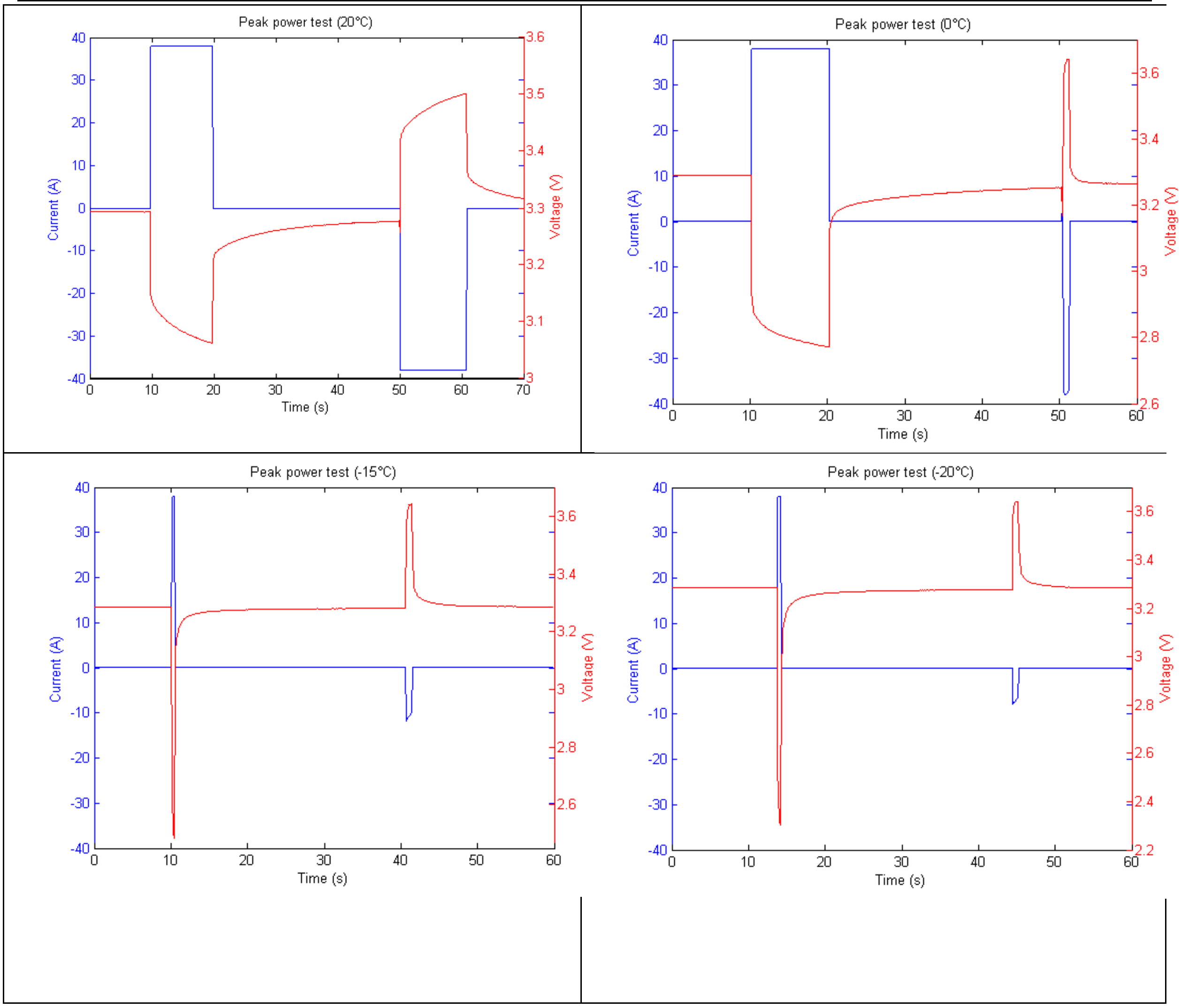

Figure 3. Results of the peak power tests at different temperatures.

As seen in Figure 3, the test was successful at 20°C. At 0°C, the cell demonstrated the required discharge capability, but was unable to charge as the cell voltage breached the upper limit of 3.6V. Both at -15°C and -20°C, the cell was unable to deliver the required power in both discharge and charge.

It is to be noted that during charge at -15°C and -20°C the current did not reach the required value of 38A, because of the voltage limitation. The charging hardware automatically limited the charge current to avoid cell damage; the charging phase is not immediately stopped so that the shapes clearly show what happens. The delay between reaching of cell voltage limitation and actual stopping of the current is around half a second.

These results have been reported at the HCV Spring meeting held in Pisa on 15-16 March 2012, in particular during the SP 3000 meeting, and specifically analysed and discussed with Magna.

Magna confirmed this, apparently unexpected behaviour, which was motivated by a dramatic reduction in capacity at low temperatures of the cells, experimentally verified in preliminary tests at Magna and was also justified by the manufacturer.
As a consequence of this behaviour, thermal management was realized by Magna, in order to avoid the occurrence of extreme (low) temperatures, outside the recommended working temperature window of the cells.

Instead, it was additionally stressed by Magna that the highest efforts should be given to determine a good SOC estimation technique, able to overcome the big threats (and safety constraints) these cells pose, because of their peculiar voltage behaviour.

It was therefore agreed upon concentrating Pisa's efforts in determining the cell's model at ordinary temperature (20°C), which is of the utmost interest for the project.

It was then agreed to determine and test the whole procedure, and subsequently extend it with experimental test results, obtained at different temperatures.

The procedure comprises:
- detailed definition of the cell's mathematical model
- detailed definition of the procedure to determine the model's numerical parameters
- detailed definition of the algorithm to estimate the battery's SOC
- verification of model and SOC-estimation algorithm quality

Verification of the applicability of the general model and determination of numerical parameters

In Deliverable D3100.5 a survey of literature about electrochemical cell mathematical models was performed, that has shown a general uniformity of the models discussed in the more recent papers, that all can be, with minor differences reproduced using the equivalent circuit shown in Figure 1.

Indeed this circuit is not able to represent the effect of self-discharge in cells; a model that could represent this effect can be one as shown in Figure 4.

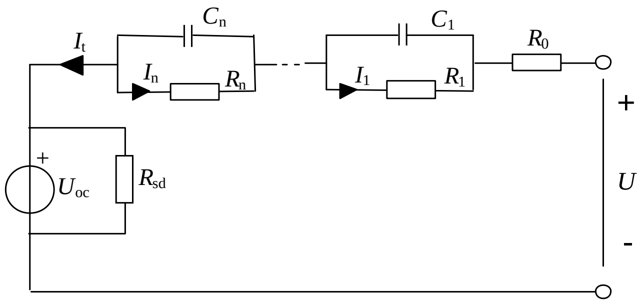

Figure 4. Model of Figure 1 with the addition of the self-discharge resistance R_{sd}.

The non-linear self–discharge resistance R_{sd}, indeed draws some current from the open-circuit voltage U_{oc}, thus causing the SOC to slowly change even when the terminal current is zero.

However, the value of this resistance is difficult to evaluate, because it depends on SOC and temperature, and influences SOC very slowly. Since one of main purposes of HCV is to closed-loop evaluate OCV, the current drawn by R_{sd} can be taken as a disturbance, and efforts can be concentrated in evaluating issues and applicability of the model shown in Figure 1, in which R_{sd} is neglected.

Although the models in Figure 1 and 4 have become almost “standard” models for electrochemical Li cells in the literature, it has been preferred and judged appropriate to first verify its suitability to the HCV cell chemistry, which has some specific features.
In particular, this model does not include any hysteresis: the numerical values of voltage sources, resistances, capacitances are intended to be function of SOC and temperature, but not on the current direction.

The Multiple Step Test (MST) sequence defined in Deliverable D3100.5 [2] came in two ways: charge-based and discharge-based.

These two ways can be used to determine all the parameters of the cell’s equivalent circuit, and the obtained values can be compared so that to verify differences in cell’s behaviour when charging and discharging.

Moreover, the mathematical model of Figure 1 has a generic number of R-C block, and the best value for *n* had to be chosen.

To determine the number of R-C blocks, to avoid excessive complexity of the model, and therefore of the procedure to evaluate the numerical values of parameters, the basic decision was made of considering for that number two options: n=1 and n=2.

Naturally with n=1 the precision is expected to be low, but also the procedure to draw parameters from experimental tests is simplified.

The procedure to evaluate all values of R_k’s and C_k’s is the one detailed in section “Technical progress | Modelling Li batteries | General” of Deliverable D3100.5 [2].
This procedure is applied to the result of the Multiple-Step-Test, at different values of SOC, and therefore values of R_k’s and C_k’s at different values of SOC are determined.

To understand the process, the results obtained when SOC=50% are discussed here.

Figure 5 shows a comparison between experimental and simulated voltages, , immediately after the end of a discharge pulse, at SOC=50%.
The blue curve shows actual values: voltage drops first fast then more slowly.

The voltage response to the same current of the considered battery model depends on the number *n* of *R-C* blocks, and the numerical values of all R_k’s, C_k’s and U_{oc}.

A procedure to identify all these values is used to minimise the error between actual and simulated voltage profile. The error function chosen is:

$$\varepsilon = \sqrt{(u_{\text{actual}} - u_{\text{model}})^2} \qquad (1)$$

The numerical values obtained after this process has been carried out are reported in Table 3.

Table 3. Numerical values of model parameters.

n	U_{oc} (V)	R_0 (mΩ)	R_1 (mΩ)	R_1C_1 (s)	R_2 (mΩ)	R_2C_2 (s)
1	3.254	2.0	7.2	132	-	-
2	3.255	1.4	5.9	22	2.0	827

Figure 5 shows the actual and simulated voltages, considering both cases (with n=1 and n=2).

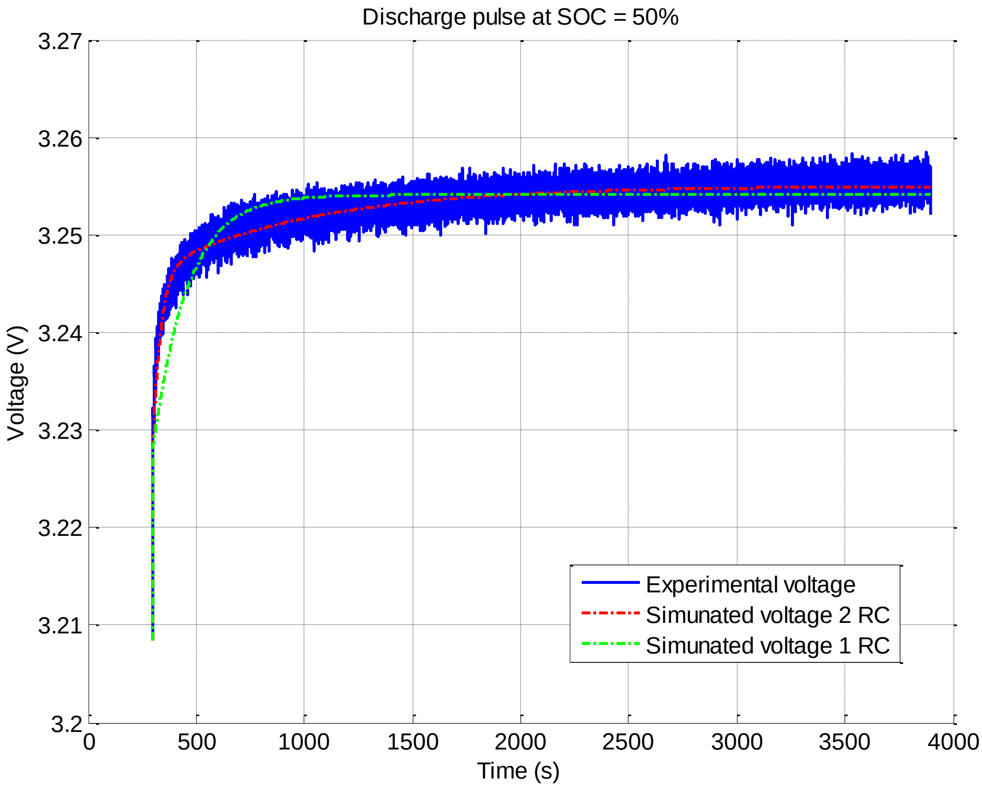

Figure 5. Voltage behaviour immediately after the end of a discharge process, while SOC=50%.
Comparison between experiment and model (R's, C's, U_{oc} determined by error minimisation).

The comparison shows that both models present rather acceptable results, while the 2-blocks one has a distinct advantage.

One detail of the results is interesting: the green curve, while it generally has a sufficiently reasonable trend, has a final value (that can be read for t=4000 s) that is markedly lower than the actual OCV, as can be inferred as the centre of the blue, experimental band.

Indeed, the value of U_{oc} is very important for further analysis and implementation of algorithms for SOC estimation. Therefore, it is advisable to force the choice of the most reasonable value of this parameter, as observable in the experimental data and then keep it as constant. This implies that the minimisation of error between experimental and model trends is made acting just on *R*'s and *C*'s, while U_{oc} is taken as being known in advance (as a constant value for the defined chemistry and model).

The corresponding result is shown in Figures 6 to 8.

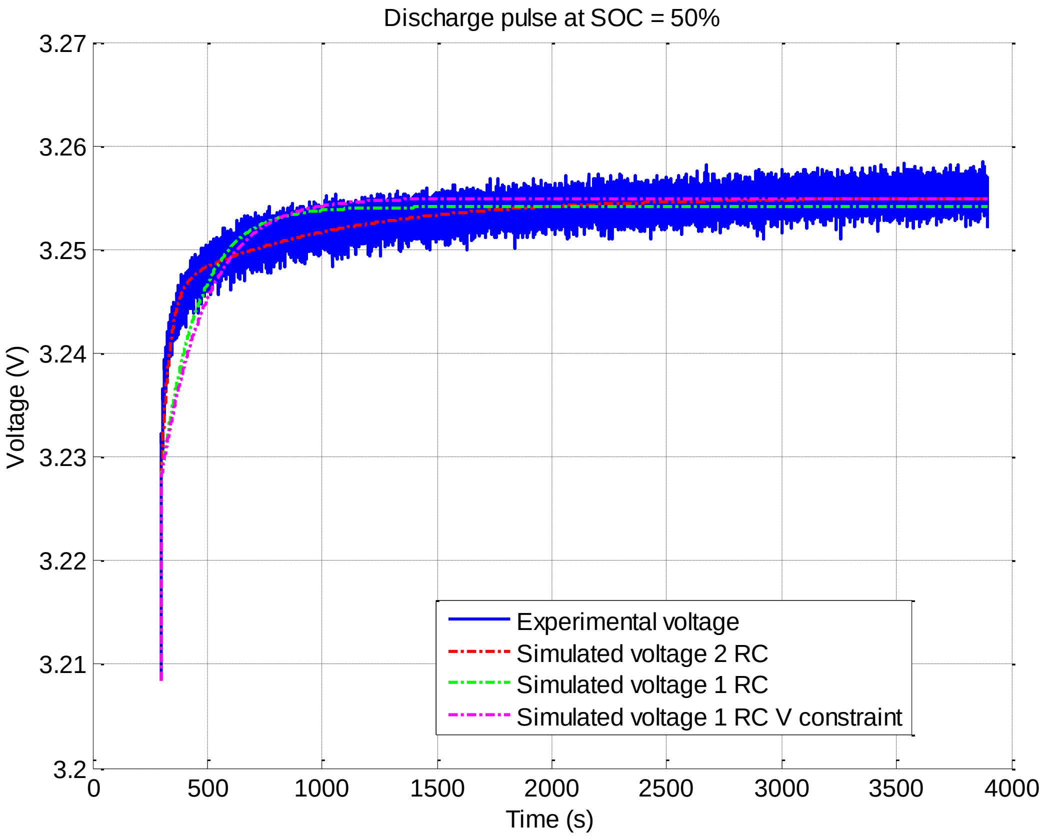

Figure 6. Voltage behaviour immediately after the end of a discharge process, while SOC=50%.
Comparison between experiment and model
(R's, C's determined by error minimisation, U_{oc} constrained).

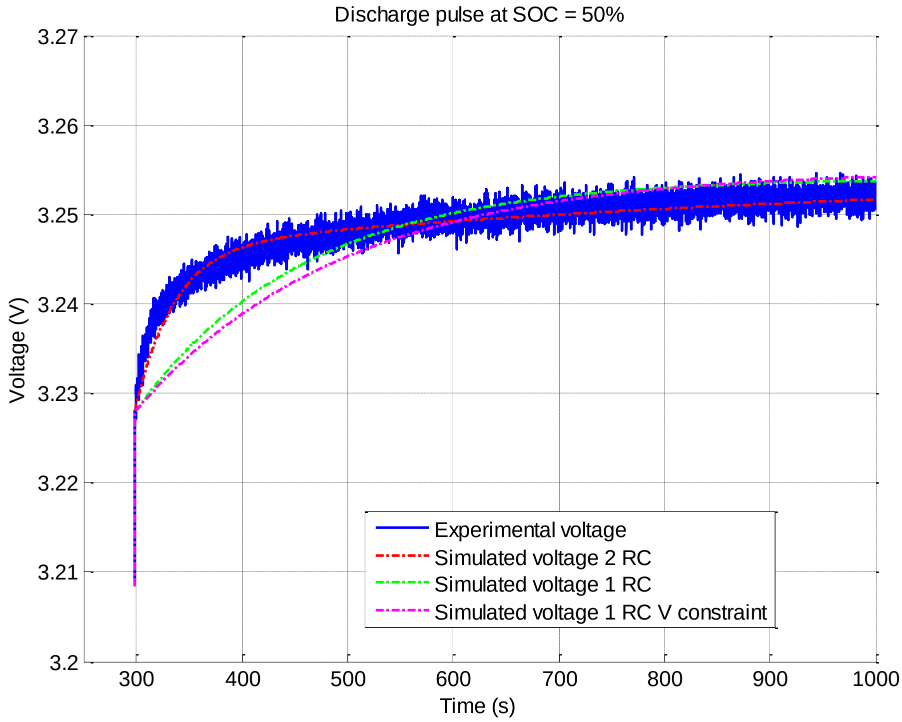

Figure 7. Expansion of the first part of Figure 6.

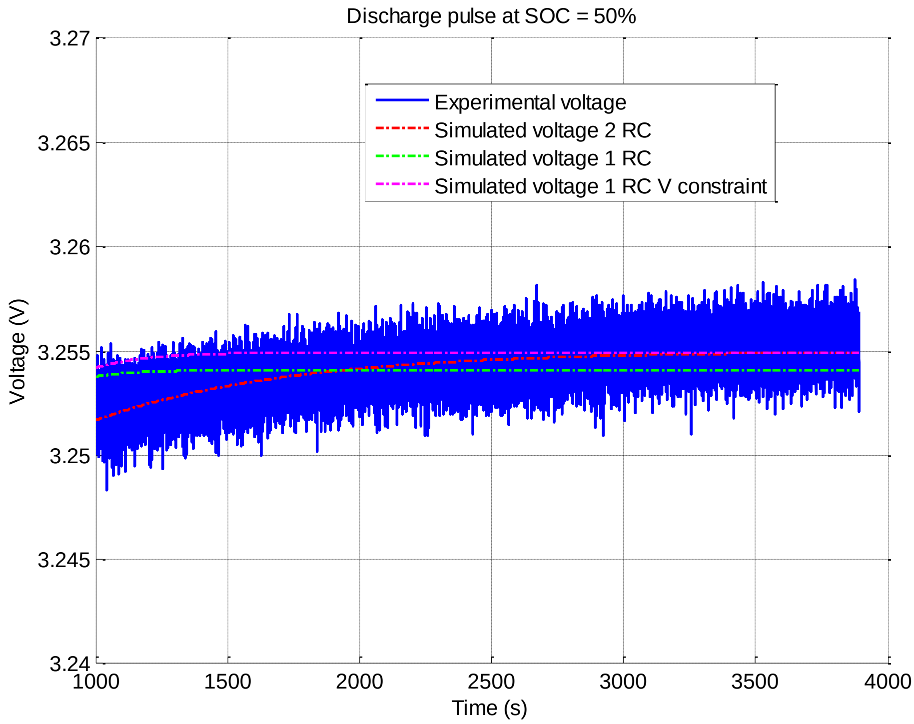

Figure 8. Expansion of the last part of Figure 6.

Figures show that the model voltage obtainable with U_{oc} constrained and n=1, is much worse than in the previous case, especially at the very beginning of the transient mode.
With n=2, on the contrary, there is no need to constrain U_{oc}, since the error-minimisation algorithm automatically gives an acceptable value for this parameter. Moreover, the 2 R-C block model gives very good results even during the first part of the considered transient condition.
It was therefore concluded that two R-C blocks are important to keep good quality of the model reproduction of experimental results, while constraining the final voltage U_{oc}. Therefore the following decision has been adopted:

Decision. The adopted model was decided to have two *R-C* blocks.

If instead we consider the charge-based MST, the result when SOC= 50% is that shown in Figure 9.

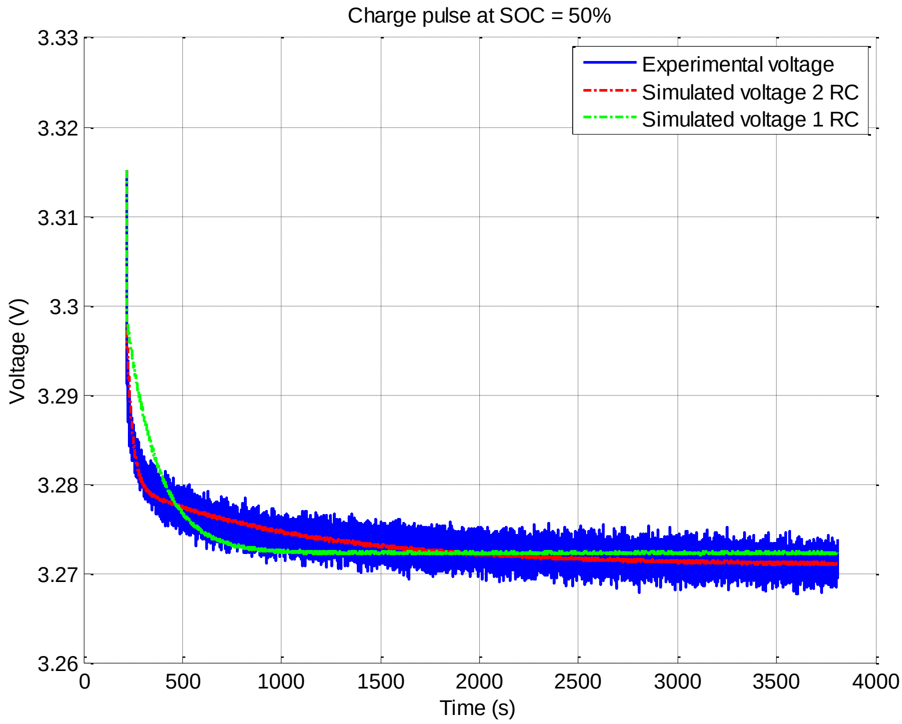

Figure 9. Voltage behaviour immediately after the end of a charge process, while SOC=50%. Comparison between experiment and model (R's, C's, U_{oc} determined by error minimisation).

The corresponding numerical parameters are presented, along with those referring to the transient after discharge, in Table 4.

Table 4. Model numerical parameters at SOC=50%, after charge and discharge processes.

Transient	U_{oc} (V)	R_0 (mΩ)	R_1 (mΩ)	R_1C_1 (s)	R_2 (mΩ)	R_2C_2 (s)
After charge	3.272	4.5	4.5	37	2.2	738
After discharge	3.255	1.4	5.9	22	2.0	827

If the procedure to identify/determine all parameters is strictly applied, all parameters have values during charge and discharge.
This duality, however, is a potential source of big difficulties, arising when the cell is subject to continuously varying currents, as in the case of hybrid vehicle applications. Indeed, if the model parameters suddenly switch from charge to discharge values whenever the current at cell's terminals changes its sign, it is not difficult to foresee large mismatches between simulation and actual values (unfitting conditions).

The basic idea, which is similar to what is often found and proposed in literature [4], is therefore of adopting hysteresis, i.e. different values after charge and after discharge only for U_{oc}, and using intermediate values for the other parameters:

Decision.
- The adopted model *R*'s and *C*'s does not depend on history except for their dependence on temperature and SOC.
- U_{oc}, instead, will have some direct dependency on the cell's history.

Consequently, the choice of resistances and capacitance values for the model at different SOC must somehow take into account what happens during charge and during discharge.

Figure 10 to 12 show the comparison of two different techniques and numerical approaches:

- Technique 1, in which the numerical values are the arithmetic mean between those obtainable during end-of-charge and end-of-discharge identification process. This technique is the simplest to implement
- Technique 2, in which the numerical values are determined by minimising the error considering both end-of-charge and end-of-discharge transients.

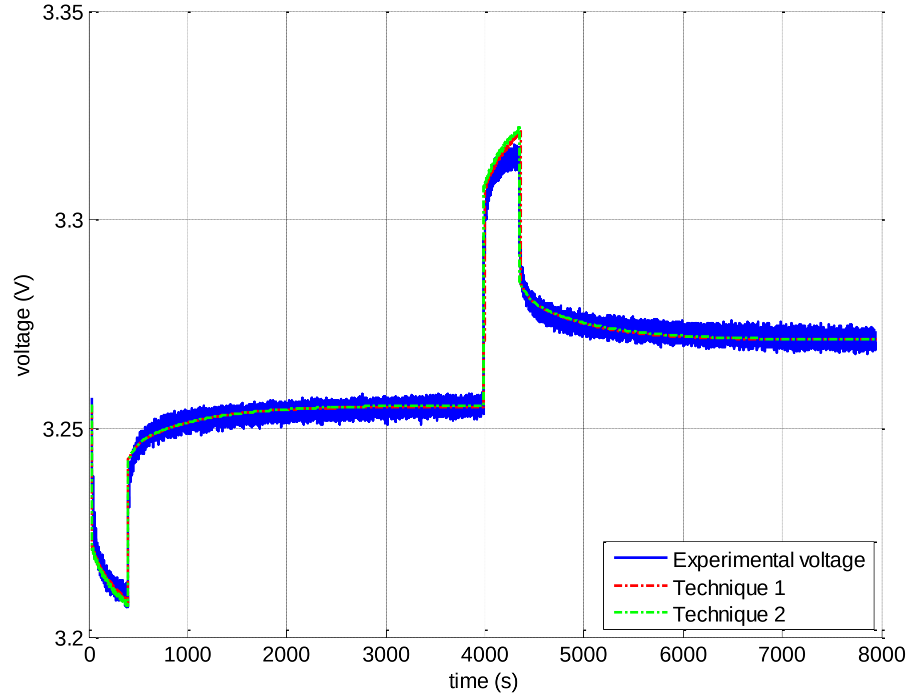

Figure 10. Comparison of voltage behaviour of models whose R-C parameters are evaluated with mean value charge/discharge (tech. 1) or global optimisation (tech. 2).

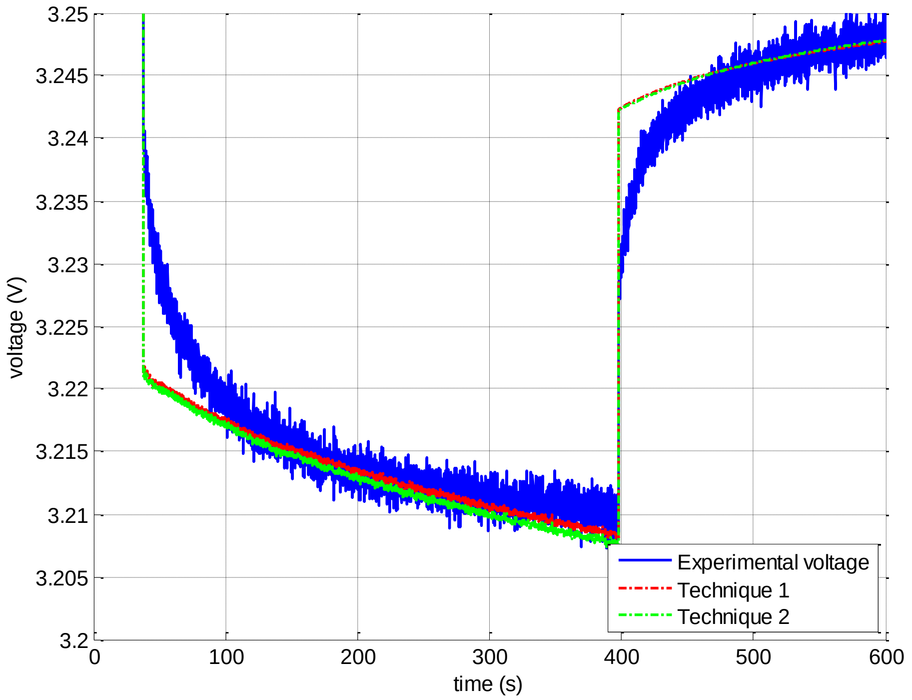

Figure 11. Expansion of left part of Figure 10.

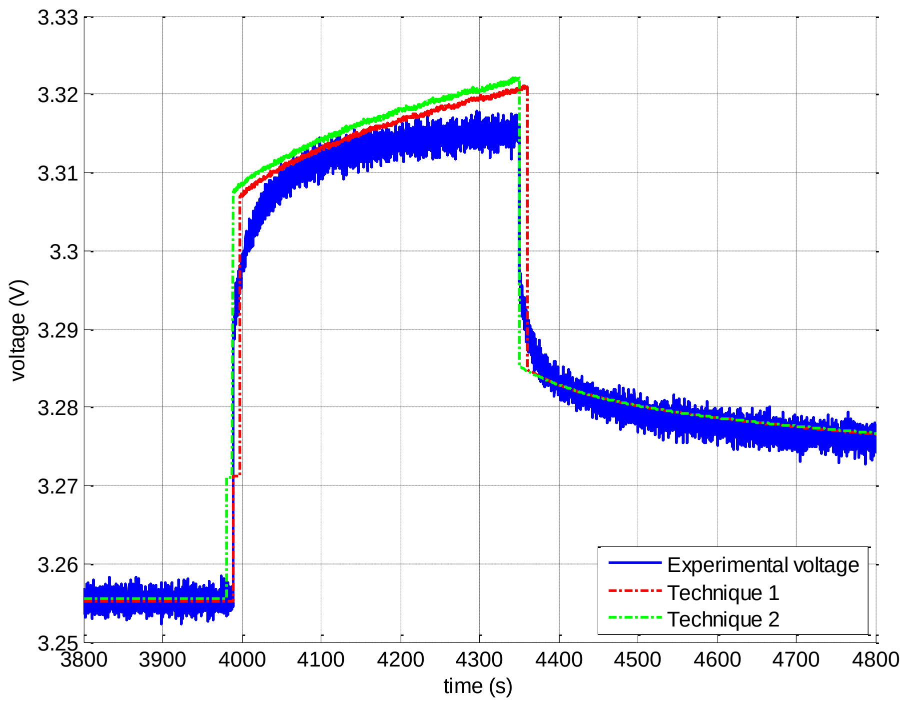

Figure 12. Expansion of right part of Figure 10.

It is apparent that the two techniques are rather equivalent. The actual implementation of evaluation of numerical parameters of the model can therefore be done in both ways.
The choice could be made considering practical issues related to the automatic determination of the numerical values from experimental tests. In fact, since it is expected that a periodical update of these values will become necessary to follow the cell (and battery) aging during the vehicle usual life, it is advisable to develop techniques/methods to identify/measure/calculate the numerical values of the model parameters in an easy and automated way.

Conclusion. The identification process of resistances and capacitances of the model can evaluate numerical values after charge or after discharge transients and take the numerical averages of the values thus obtained.
As an equivalent alternative, these values can be obtained by global error minimisation process during both charge and discharge modes.

Just for completeness, Figure 13 shows current and voltage during the MST tests (both charge-based and discharge-based).

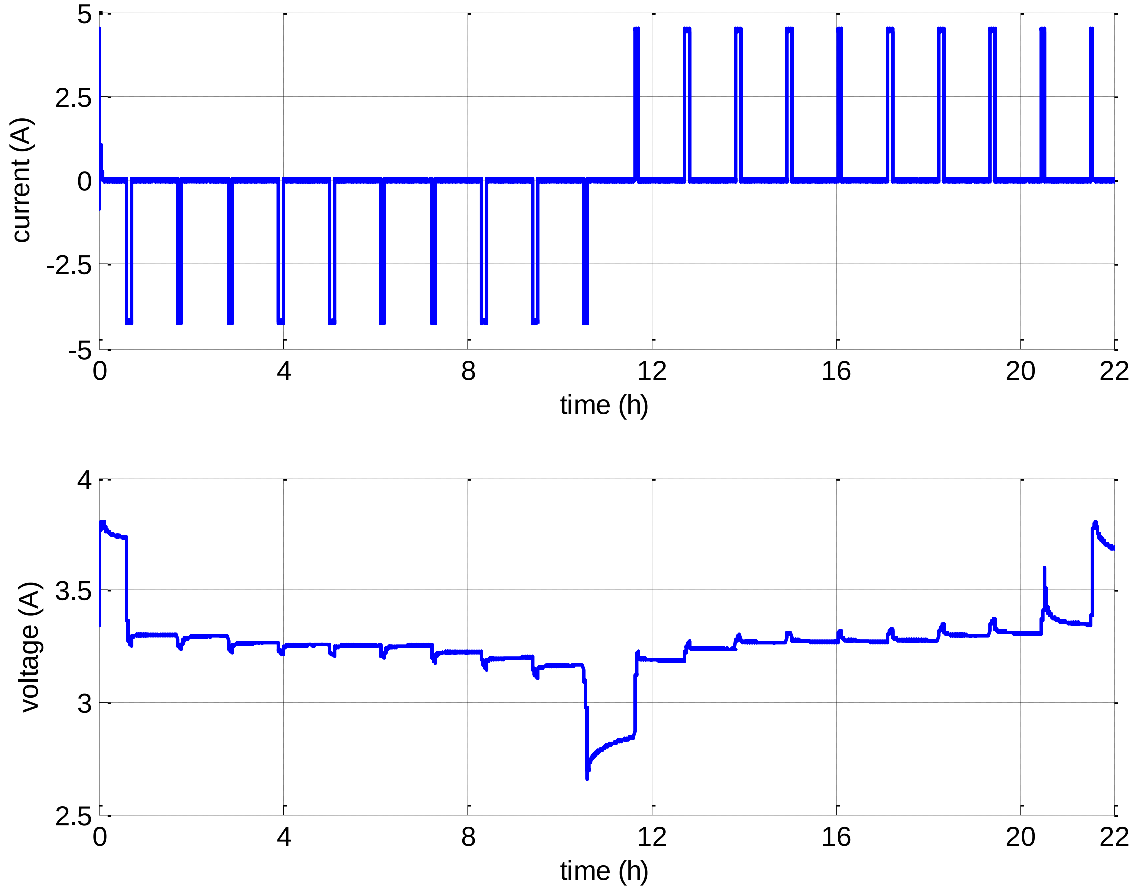

Figure 13. Current (above) and voltage profiles as measured during MST: discharge-based (up to t=10 h) and charge-based (above t=10h).

Determination of the five parameters (R_0, R_1, C_1, R_2, C_2) has been performed in this way at various values of SOC. The results obtained are displayed in Figure 14 to Figure 17.

Finally, Figure 18 shows the U_{oc} values. They are two per each SOC value: one as obtained during the discharge-based MST, and the other during the charge-based MST.

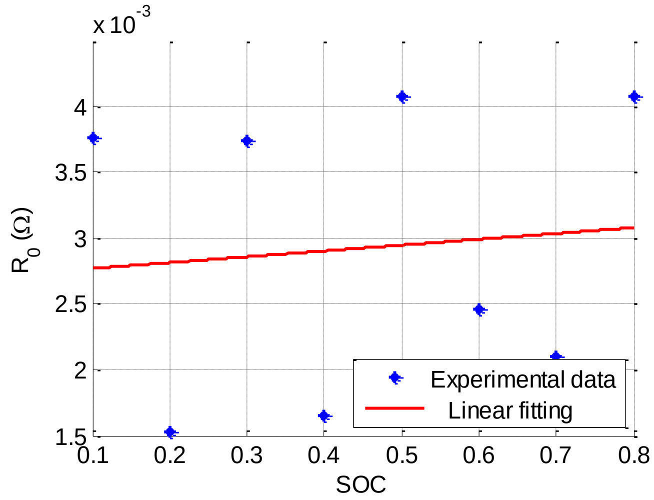

Figure 14. Experimental data on R_0 and linear interpolation.

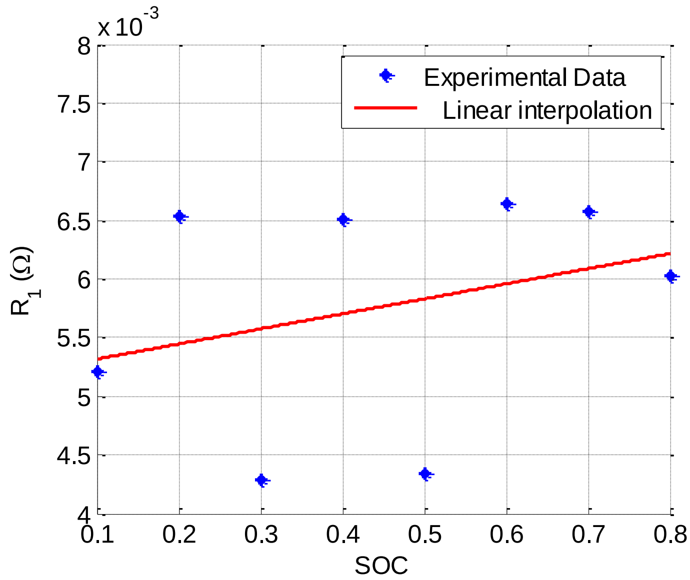

Figure 15. Experimental data on R_1 and linear interpolation.

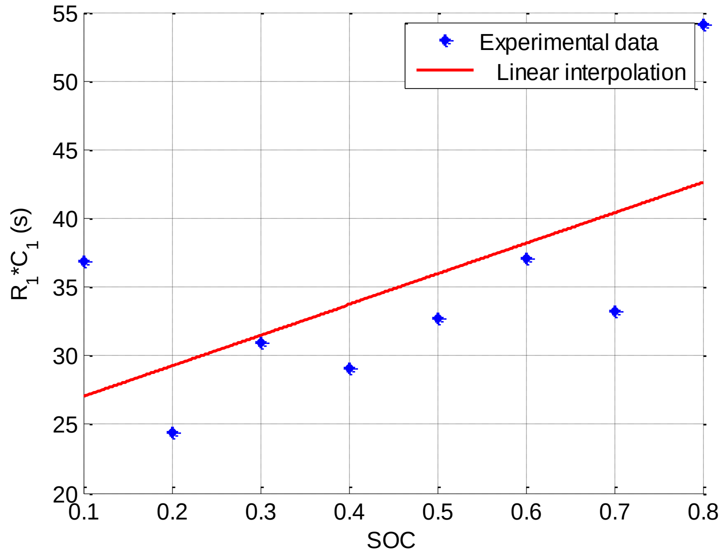

Figure 16. Experimental data on time constant R_1C_1 and linear interpolation.

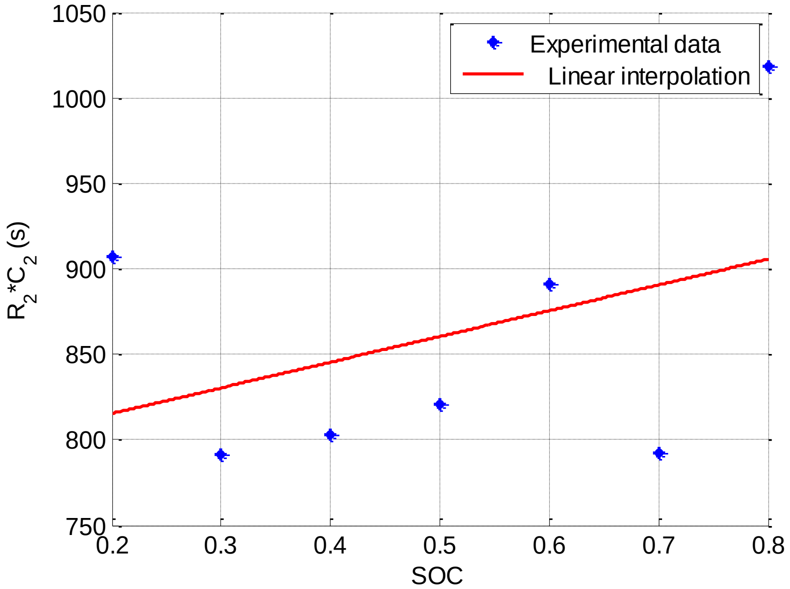

Figure 17. Experimental data on time constant R_1C_1 and linear interpolation.

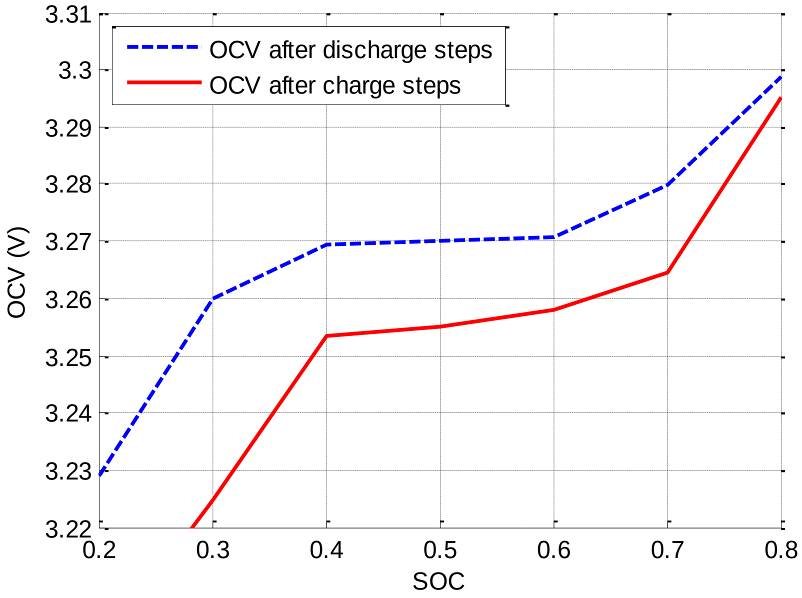

Figure 18. Experimental data on voltage U_{oc}, after discharge steps and after charge steps.

Discussion

The application of parameter identification procedure to the experimental results of the MST sequence on the HCV Li cells has allowed a correct evaluation of numerical values for R_0, R_1, C_1, C_2 and U_{oc} as a function of SOC.

Some of the parameters, especially R_0 and R_1, showed an unclear trend over SOC. The quasi-oscillatory behaviour that can be seen in experimental data of Figure 14 and Figure 15 cannot be easily explained in terms of the cell's physics.

The most likely reason for this behaviour is that the minimum of error is rather flat over individual variations of the parameters, and therefore the numerical minimisation algorithm finds values that experience large variation, even though there is not a precise physical (or chemical) meaning for this.

It is not necessary, however to find an analytical formula to interpolate the plots of parameters R_0, R_1, C_1, R_2, C_2. To ease the ability of an easy automation of parameter extraction from experimental tests, it is simpler to make linear interpolation or spline interpolation between the values outputted by the error minimisation algorithm. This will be used in the SOC evaluation algorithm that will be discussed in deliverable D3200.7.

An equivalent representation of the same model as in Figure 4, explicitly showing the dependence of U_{oc} on the SOC is shown in Figure 19.

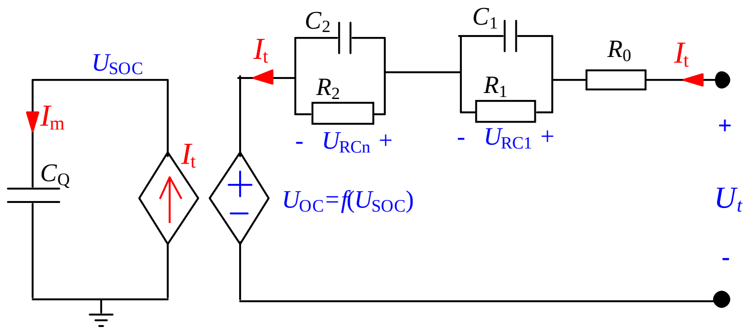

Figure 19. Cell model with 2 R-C blocks (form 2).

In the left circuit here U_{SOC} is a voltage; however its numerical value is equal to SOC, since it becomes one when the cell is completely full. C_Q is the capacitance of the capacitor shown in the circuit, but its value is the cell's capacity in Ah.
Since this representation gives greater evidence to SOC, which is the objective of the algorithm to be introduced in this section, this graphical representation of the cell and the corresponding symbols are adopted.

From this circuit the following equations are used:

$$\begin{cases} \dot{U}_{SOC} = \dfrac{-U_{SOC}}{R_{sd} C_Q} + \dfrac{1}{C_Q} I_t \\ \dot{U}_{RC1} = \dfrac{-U_{RC1}}{R_1 C_1} + \dfrac{1}{C_1} I_t \\ \dot{U}_{RC2} = \dfrac{-U_{RC2}}{R_2 C_2} + \dfrac{1}{C_2} I_t \\ U_t = U_{OC} + R_0 I_t + U_{RC1} + U_{RC2} \end{cases} \quad (2)$$

Note that they are written leaving U_{oc} "as is", since its value is evaluated separately, as described in the previous section.

Equations (2) can be written in discrete form as follows:

$$\begin{cases} \boldsymbol{x}_{k+1} = \boldsymbol{A}\boldsymbol{x}_k + \boldsymbol{B}\boldsymbol{u}_k \\ \boldsymbol{y}_k = \boldsymbol{C}\boldsymbol{x}_k + \boldsymbol{D}\boldsymbol{u}_k \end{cases} \qquad \begin{cases} \boldsymbol{u} = [I_t] \qquad \boldsymbol{x} = [U_{RC1} \quad U_{RC2}]^T \qquad \boldsymbol{y} = [U_t - U_{oc}] \\ \boldsymbol{A} = \begin{bmatrix} e^{-t/R_1C_1} & \\ & e^{-t/R_2C_2} \end{bmatrix}; \quad \boldsymbol{B} = \begin{bmatrix} R_1\left(1-e^{-t/R_1C_1}\right) \\ R_2\left(1-e^{-t/R_2C_2}\right) \end{bmatrix} \\ \boldsymbol{C} = [1 \quad 1]^T \qquad \boldsymbol{D} = R_0 \end{cases} \quad (3)$$

The vector of state variables ***x*** is constituted by the two voltages across *R*-*C* blocks.
As usual, matrix ***A*** represents the dynamic evolution of state ***x***, matrix ***B*** indicates the quota of input directly transferred to states (algebraic part of *R*-*C* blocks) and matrices ***C*** and ***D*** indicate the influence of state and input into output, constituted by the battery's voltage at its terminals.

Conclusions

This deliverable has dealt with all the practical issues encountered when defining and implementing in practice a suitable mathematical model for the HCV's lithium cell.

Based on the decisions taken during discussions mainly with Magna and on the results of experimental tests on cells, attention was concentrated towards the behaviour at room temperature.
Test results were produced at the University of Pisa's laboratories, were analysed and then discussed to select and validate the selected model.
Suitable numerical values for all the model parameters have been determined, and the mathematical equations of the model written.

This model has been used as the basis for SOC estimation and algorithm development, as detailed in Deliverable D3200.7 [1].

References

1. Hybrid Commercial Vehicle (HCV) FP7-Project, "Algorithm for Li cell, D3200.7," University of Pisa, 2013.
2. Hybrid Commercial Vehicle (HCV) FP7-Project, "Modelling Test Matrices for Li batteries and SC, D3100.5," University of Pisa, 2012.
3. Hybrid Commercial Vehicle (HCV) FP7-Project, "Preliminary model definition for Li cell, D3200.5," University of Pisa, 2013.
4. Z. Hanlei; C. Mo-Yuen, "On-line PHEV battery hysteresis effect dynamics modeling," IECON 2010 - 36th Annual Conference on IEEE Industrial Electronics Society, pp.1844-1849, Nov. 7-10 , 2010, doi: 10.1109/IECON.2010.5675395.